JOINT INSTITUTE FOR NUCLEAR RESEARCH
Frank Laboratory of Neutron Physics

FINAL REPORT ON THE SUMMER STUDENT PROGRAM

Q-space conversion by time-of-flight using silver behenate

Supervisor:
Dr. Alexander I. Kuklin

Student:
Roman Moryachkov, Russia
Kirensky Institute of Physics

Participation period:
July 28 – August 24

Dubna, 2018

Table of contents

Abstract

Impulse regime of the neutron beam generating to the measurement facilities is developed on the IBR-2 reactor at JINR, Dubna. According to this there is possibility to apply a Time-Of-Flight (TOF) technique experiments with neutrons. In particular, the small-angle neutron scattering (SANS) data acquisition is used on the SANS spectrometer YuMO, which utilizes the TOF measurements with two ring detectors. Each detector consists of 8 separate rings working with own timer, which allows to calculate the neutron wavelength depended on time of flight of those neutrons to the detector. On this basis the conversion is performed from the measured parameters of scattering angle with the number of counts at definite time into the reciprocal space with the coordinate Q and intensity of signal. Parameter Q gives the absolute value of the amplitude of the coherent scattering independently of the wavelength of the received radiation. To perform the appropriate conversion TOF data to the Q-space of parameters it is necessary to take into account the equipment physical parameters, nature and form of measured signal. In this work we have attempted few approaches for the processing of the data from YuMO spectrometer with the sample of silver behenate to convert it into Q-space on each ring separately and compare results with data obtained by the SAS program.

Introduction

To understand how biological macromolecules specifically interact with other molecules and exercise the catalytic activity it is necessary to know their structure. There are several methods of structural biology which can reconstruct the tertiary structure of biomolecules. The nuclear magnetic resonance (NMR) allows to solve the structure of biomolecules in solution, but it requires the isotopic labeling of the sample and this method is limited by size of molecule [1]. The X-ray diffraction (XRD) as well as NMR allows to get the structural information with high resolution, but XRD needs the crystal [2]. Many proteins and single-stranded DNA/RNA cannot be crystallized and it is the challenge to obtain the periodic structure from their solution [3] .

To study the biological macromolecules in solution the small-angle scattering methods are used and these methods become increasingly popular in structural biology [4,5]. Small-angle X-ray scattering (SAXS) is the elastic scattering of X-rays on the electron density of the biomolecules chaotically floating in solution. This method allows one to work with nanoparticles with size 1 - 1000 nanometers (10 kDa - 10 MDa) and to obtain without crystallization the structural parameters of biomolecules such as maximal dimension, radius of gyration, distance distribution inside the molecule and also to reconstruct the shape of the macromolecule with low resolution and intramolecular domain or intermolecular ligand arrangement.

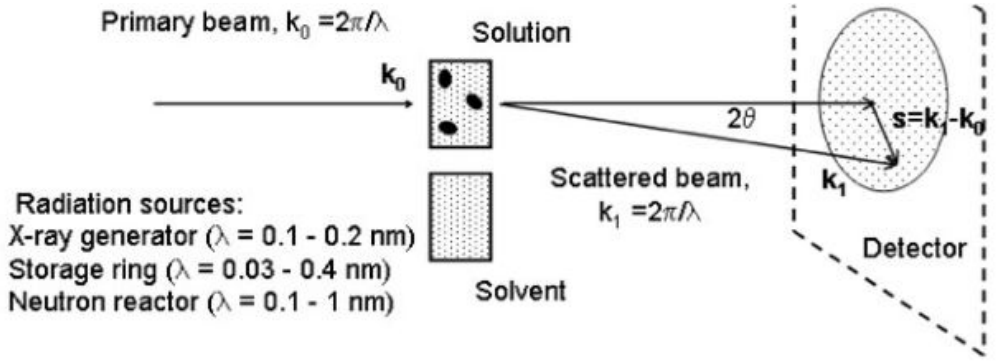

Fig. 1 - Scheme of the SAS experiment. λ is the wavelength, s - momentum transfer. Sample SAS measurement is followed by solvent scattering with further background subtraction and radial averaging respectively the direct beam.

Scattering momentum transfer is described by equation:

$$Q = \frac{4\pi \, sin\,(\theta/2)}{\lambda}, \qquad (1)$$

where θ is an angle between incident and scattered beam, λ is the wavelength (X-ray or neutron).

The experimental data set and data reduction in SANS method is not differ from SAXS, but the scattering process has principal features [6]. The thermal neutron scattering occurs on the atomic nuclei density against the electron density in SAXS, and depends on the isotopic composition of the substance under investigation and magnetic properties of the sample. These

features give additional advantages with using this method. For example, atomic nucleus of deuterium $^{2}H(D)$ has the amplitude of coherent scattering +0,667 (10^{-14} m), whereas for the protium nucleus ^{1}H this value is -0,374 (10^{-14} m).

According to noted above, the contrast variation method is used in SANS experiments . It allows to investigate the spatial structure of the complexes consisted of macromolecules with different neutron scattering length density (SLD) [7], for example protein - nucleic acid complexes.

Using various proportion of “lite” and “heavy” water in series of experiments, it is possible to achieve the match of SLD for the deuterium buffer and one of the component of the complex and then with the second component. Using contrast variation one sample can give as minimum three different scattering curves, which provide us information about conformational changes and interactions in the macromolecular complexes.

YuMO - small angle neutron scattering spectrometer

All neutron investigations in JINR are based on the work of the high-flux impulse reactor IBR-2. Reaktor does not generates constant high neutron stream, but provide portions of powerful neutron beams with intensity ~10^{16} n/cm^2/c with the power 2 MW, frequency of the impulses is 5 and 10 Hz, pulse half-width is 200 μs.

The YuMO facility provides the time-of-flight (TOF) technique [8,9]. The wavelength of the scattered neutron depends on the time after the impulse start. It gives the redundancy of data, because of each time interval we would have the scattering pattern on different wavelength.

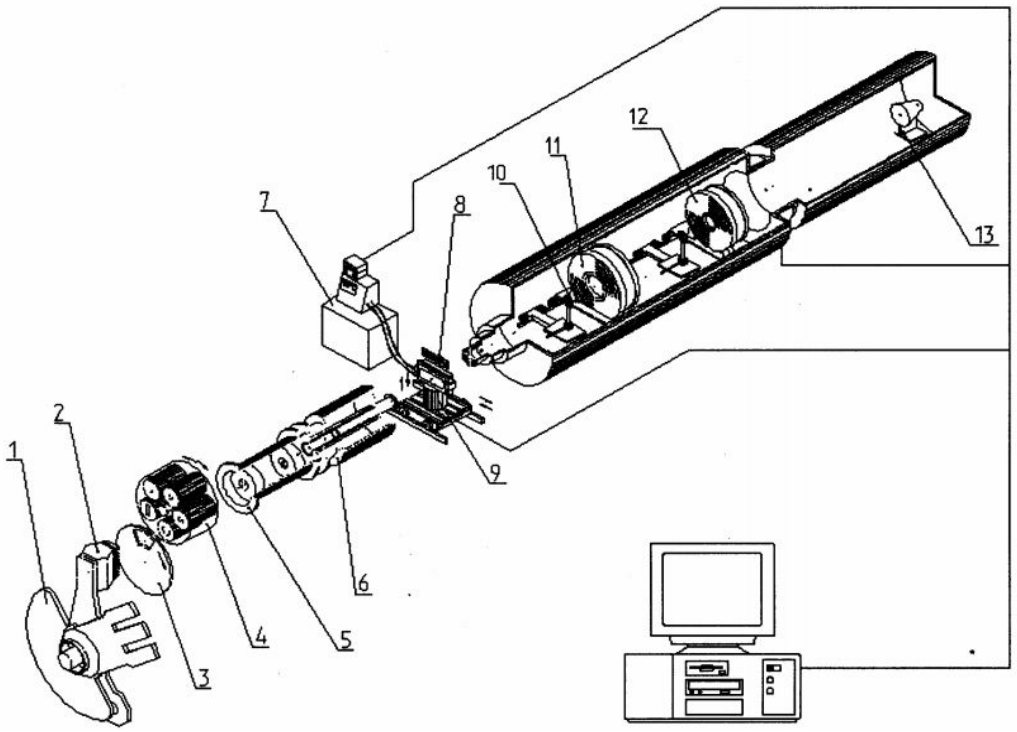

Fig. 2 - YuMO facility on the IBR-2 reactor (4th channel). 1 - main and auxiliary moveable reflectors, 2 - reactor active zone with the moderator, 3 - interrupter, 4 - changeable collimator, 5 - vacuum tube, 6 - adjustable collimator, 7 - thermostat, 8 - plate with the samples, 9 - table for

samples, 10 - vanadium standard, 11,12 - ring detectors (“OLD” and “NEW” correspondingly), 13 - direct beam detector.

Each detector “OLD” and “NEW” consists of 8 rings, each ring is vapor ^{3}He detector, width ~3 cm, moderator-detector distance for “OLD” is 22.525 m, for “NEW” - 30.990 m. Diameter of the “OLD” detector is about 70 cm, “NEW” - 50 cm.

Geometry of the YuMO spectrometer is changed periodically for different tasks. Hence it is necessary take into account these changes for the correct data processing, structure parameter calculations and conversion scattering data to reciprocal space in the coordinates I(Q), where I is intensity of the scattered neutron beam, Q - momentum transfer.

Time-of-flight method

As the thermal neutron speed is not high, it is possible to analyze the neutron wavelength by time of flight [10]. With known reactor moderator - sample distance and time after impulse start, it is possible to define the wavelength of registered neutron:

$$\lambda = \frac{ht}{mL}, \tag{2}$$

where λ is the neutron wavelength, h - Plank constant, t - time of flight, m - neutron mass, L - flight distance. If we use for the wavelength the unit Angstrom, for time - milliseconds and for distance - meters, the equation can be described as:

$$\lambda = 3.958\frac{t}{L}. \tag{3}$$

SAS - package for small-angle neutron scattering data treatment

The program package SAS was developed for the preliminary SANS data processing [11]. The possibility of the simultaneous observation the data from the all rings of both detectors “OLD” and “NEW” is realised.

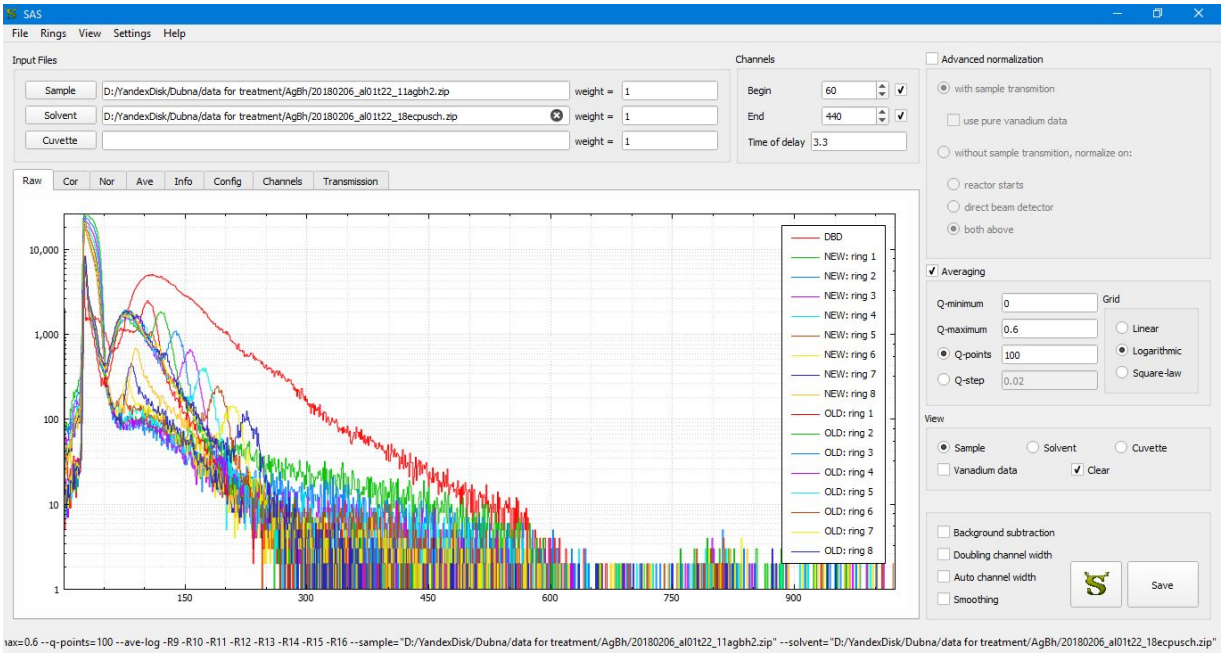

Fig. 3 - Scattering patterns of AgBh from all of 16 rings of both detectors "OLD"and "NEW" of the YuMO spectrometer. Screenshot from SAS program is presented.

Raw files received from spectrometer consist of dependencies channel number against counts for the all detectors. Program for the preliminary SANS data treatment should convert 1) a channel number into the wavelength and then into the neutron momentum transfer, and 2) detector counts into the coherent scattering cross-section. The first task is solved by the calculation of the channel number into the time of flight and then, with known moderator-detector distance and sample-detector distance and a radius of the corresponding ring, into the momentum transfer. The second task requires the additional experiment with the standard scatterer. For example, a water can be used for this purpose. The feature of the YuMO spectrometer is not only the axial-symmetric geometry and aperture in the central part of detectors for the direct beam transmission, but also the standard scatterer presence (metallic vanadium), which helps to perform the absolute calibration of the scattering cross-section with the systematic inaccuracy lower 10%. It gives the possibility to perform the preliminary experimental data treatment directly in absolute intensity scale.

AgBh calibration

For the calibration of the facility, definition of the sample-detector distance and correct transmission to the Q-space the standard Silver Behenate (AgBh) is used [9,12]. The chemical formula of AgBh is $[CH_3(CH_2)_{20}COOAg]$. AgBh is the silver salt of the long-chain fatty acid with the long-period spacing d_{001}=58.378(8) Å.

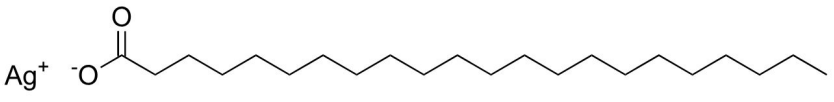

Fig. 4 - Chemical structure of silver behenate.

AgBh was used in this work as the standard for the conversion the data from counts-channel number coordinates to the intensity-Q-space. The first three Bragg peaks has the coordinates in Q-space:

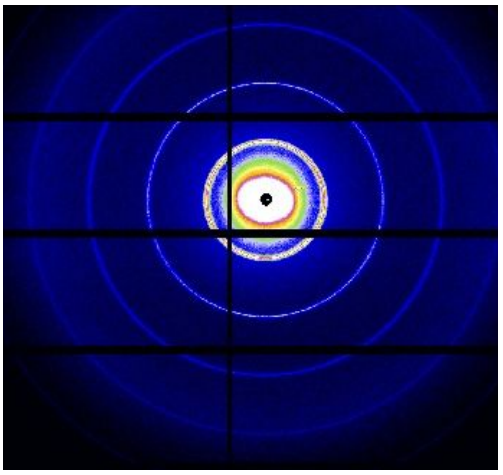

1 - 0.1076 $Å^{-1}$;
2 - 0.2152 $Å^{-1}$;
3 - 0.3228 $Å^{-1}$.

The first Bragg peak was used as the point for conversion into I(Q) coordinates.

Fig. 5 - Bragg peaks from AgBh powder diffraction.

Baseline subtraction

The Bragg peaks from AgBh scattering interfer often with the Maxwell distribution of the spectrum of thermal neutrons and irregular non-zero background scattering, which can shift the Bragg peak location on the channel axis and respectively on the absolute values in Q-space. For minimization of these factors the BaseLine subtraction (BSL) was performed to align the background level [13,14]. Data from 1 to 8 rings of the "OLD" detector and 5-8 rings of the "NEW" detector were used for the processing. Data from 1-4 rings of the "NEW" detector were excluded due to absence of the observable diffraction peak from AgBh, that is shown on the Figure 6.

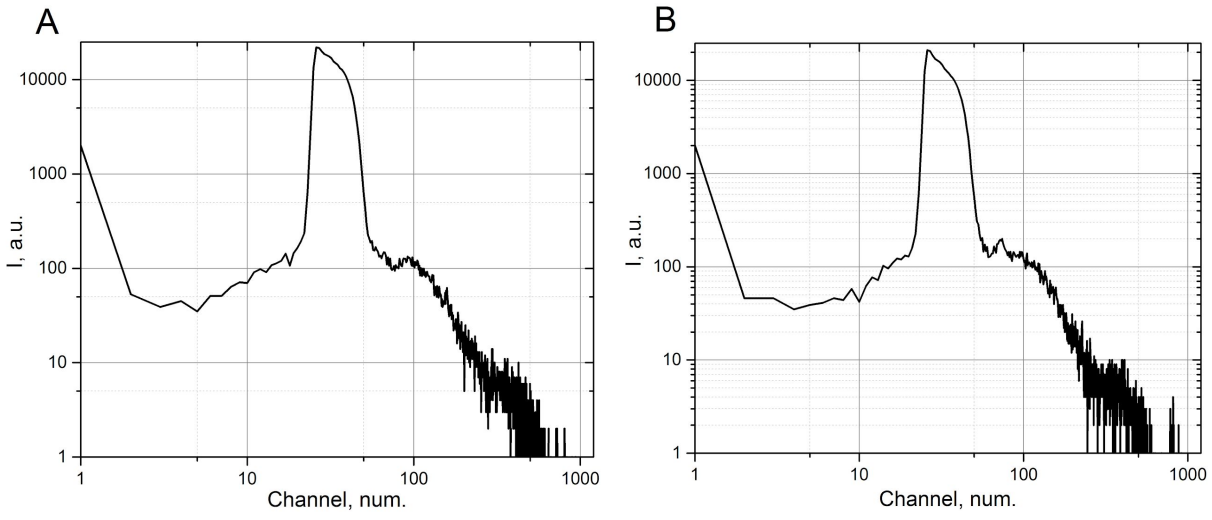

Fig. 6 - Comparison of the scattering curves for 4 (A) and 5 (B) rings of the "NEW"detector. The Maxwell signal distribution is shown on the center of these curves and the first Bragg peak is observed on the right graph part on the channel 73 for the 5th ring and is not observed for 4th ring.

The BaseLine definition and subtraction were performed in the Origin package with the function “Peak Analyzer”. The Baseline was created using method of 2nd derivative by 8-10 points and with the interpolation method “Line” or “Spline” for different scattering patterns.

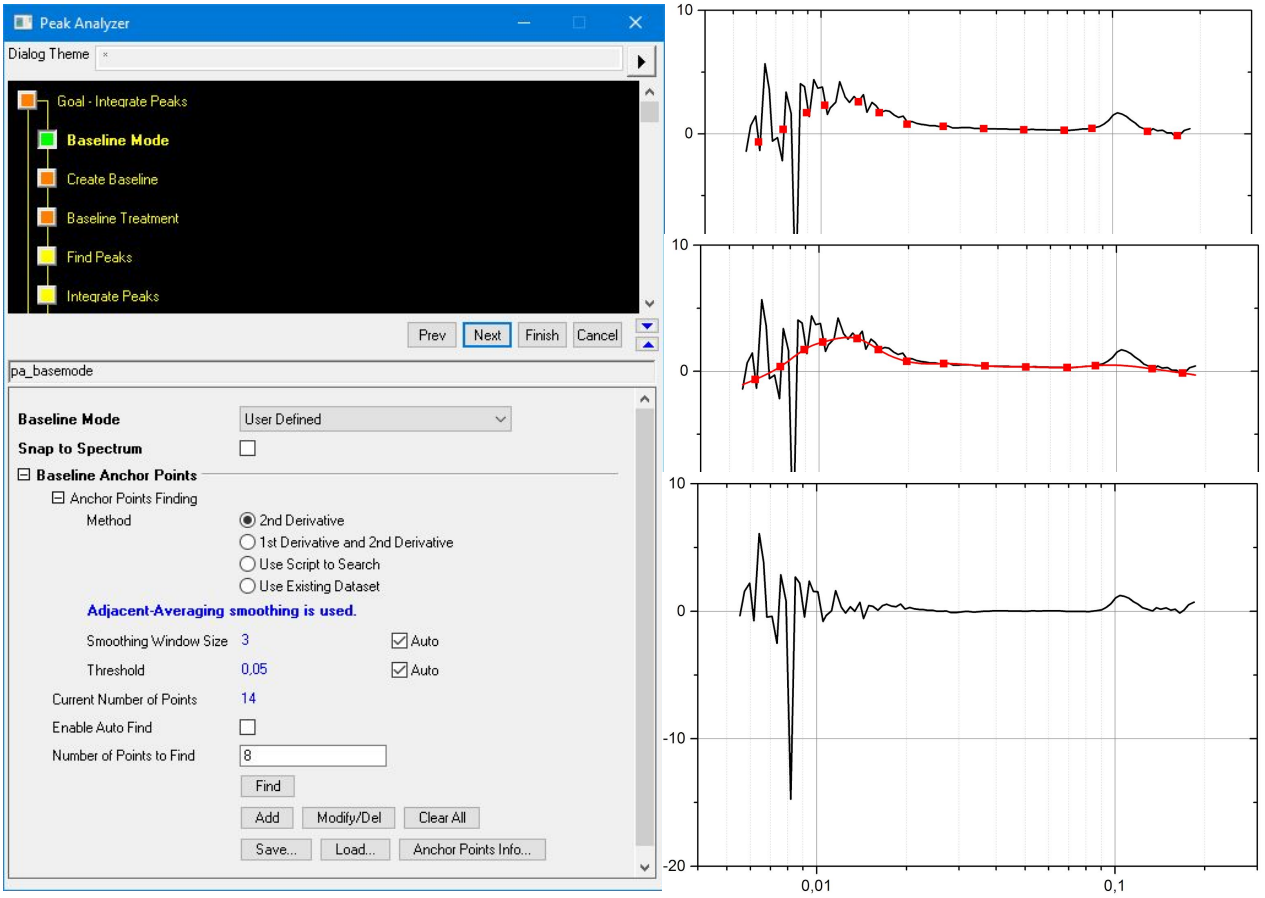

Fig. 7 - BaseLine subtraction in the Origin package.

After the background alignment using the subtraction of baseline, we can fit the Bragg peak by Gaussian peak function using the function “Multiple Peak Fit”. This approach allows to define more precisely the Bragg peak place on the axis of channels.

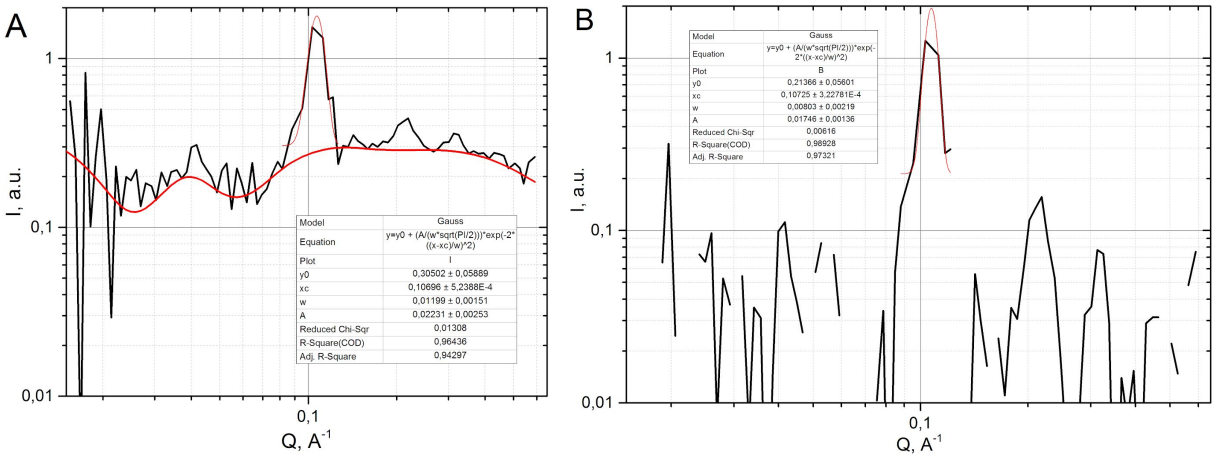

Fig. 8 - Comparison of the Gaussian fit to Bragg peak before Baseline subtraction (A) and after one (B). There is shift of the Q-value of the peak connected with the background alignment and can influence on the final Q-space definition.

Program listing

For the conversion channel number to the time of flight and the wavelength and calculation the Q value for the Bragg peak point on the basis of preliminary baseline subtraction and Gaussian fitting the short program was developed on the Python:

```
import math
#Constant data
OLD1=0.138
OLD2=0.168
OLD3=0.198
OLD4=0.228
OLD5=0.2585
OLD6=0.289
OLD7=0.319
OLD8=0.349
NEW1=0.075
NEW2=0.0955
NEW3=0.1165
NEW4=0.1375
NEW5=0.158
NEW6=0.179
NEW7=0.2005
NEW8=0.2215
reac_samp_dist=18025
reac_OLD_dist=22525
reac_NEW_dist=30990
#Before Baseline alignment
told1,told2,told3,told4,told5,told6,told7,told8 = 105,120,138,155,172,190,208,225
tnew5, tnew6, tnew7, tnew8 = 73, 79, 84, 90

#After Baseline alignment
told1,told2,told3,told4,told5,told6,told7,told8 = 105, 122, 139, 156, 173, 191, 209, 226
tnew5, tnew6, tnew7, tnew8 = 73, 78, 84, 90

#Changeable data
L=reac_NEW_dist
time=90
ring=NEW8
#Calculations
Lamb=3.958*(time*128-3300)/L
theta=math.atan(ring/((L-reac_samp_dist)/1000))
q=4*math.pi*math.sin(theta/2)/Lamb
```

print('Lamb =', float("{0:.4f}".format(Lamb)), '; theta =', float("{0:.4f}".format(theta)), '; q =', float("{0:.4f}".format(q)))

The format of the Output is presented below:
Lamb = 1.0498 ; theta = 0.0171 ; q = 0.1022

Results

Files "20180206_al01t22_11agbh2", "20180206_al01t22_18ecpusch" and "20180206_al01t22_19eb" were used for calculations, which contain AgBh scattering pattern, scattering of the capillary with buffer and the empty capillary correspondingly.

All scattering patterns from 16 rings of both detectors are presented in Figure 6. The Bragg peaks are placed on different time points due to different wavelength, on which scattering patterns were collected by YuMO spectrometer.

Averaging of the all scattering patterns in the space I(Q) based on the data from rings 1-8 of the "OLD" detector and rings 5-8 of the "NEW" detector results in the graph in SAS program shown on the Figure 7(A). The Baseline is created on the principles, described above in the "Baseline subtraction" chapter, with the "Spline" method, Q-values for the first Bragg peak before and after Baseline subtraction are presented in the Table 1.

Table 1 - Average Q values for the first Bragg peak for AgBh. Values are collected from SAS program (directly in Q-space), average values from "OLD" and "NEW" detectors before Baseline subtraction and after.

Source of data	Q value before Baseline	Q value after Baseline
SAS	0.107(2)	0.107(1)
OLD	0.109(2)	0.108(3)
NEW	0.100(8)	0.101(3)

Channel number values are obtained for each scattering pattern separately with presence of observed Bragg peaks in coordinates of the detector ring counts and channel numbers. Baseline subtractions and fitting of Gaussian envelope were performed in each case. The average Q-value was calculated for both detectors and noted in the Table 1. The discrepancies between certain detector ring values after baseline subtraction and mean values for "OLD" and "NEW" detectors are listed in the Table 2.

Table 2 - Q-values for the first Bragg peak of the AgBh scattering on each ring of detectors "OLD" and "NEW", where this peak is observable.

Ring number of "OLD" detector	Q value after baseline alignment (Δ of mean)	Discrepancy between Q_{exp} and Q_{abs} for detector "OLD"	Ring number of "NEW" detector	Q value after baseline alignment (Δ of mean)	Discrepancy between Q_{exp} and Q_{abs} for detector "OLD"
1	0,1081(-0.0002)	0.0005	1	-	-
2	0,1083(0)	0.0007	2	-	-
3	0,1084(+0.0001)	0.0008	3	-	-
4	0,1085(+0.0002)	0.0009	4	-	-
5	0,1088(+0.0005)	0.0012	5	0,0992(-0.0021)	
6	0,1084(+0.0001)	0.0008	6	0,1016(+0.0003)	
7	0,1078(-0.0005)	0.0002	7	0,1021(+0.0006)	
8	0,1079(-0.0004)	0.0003	8	0,1022(+0.0007)	

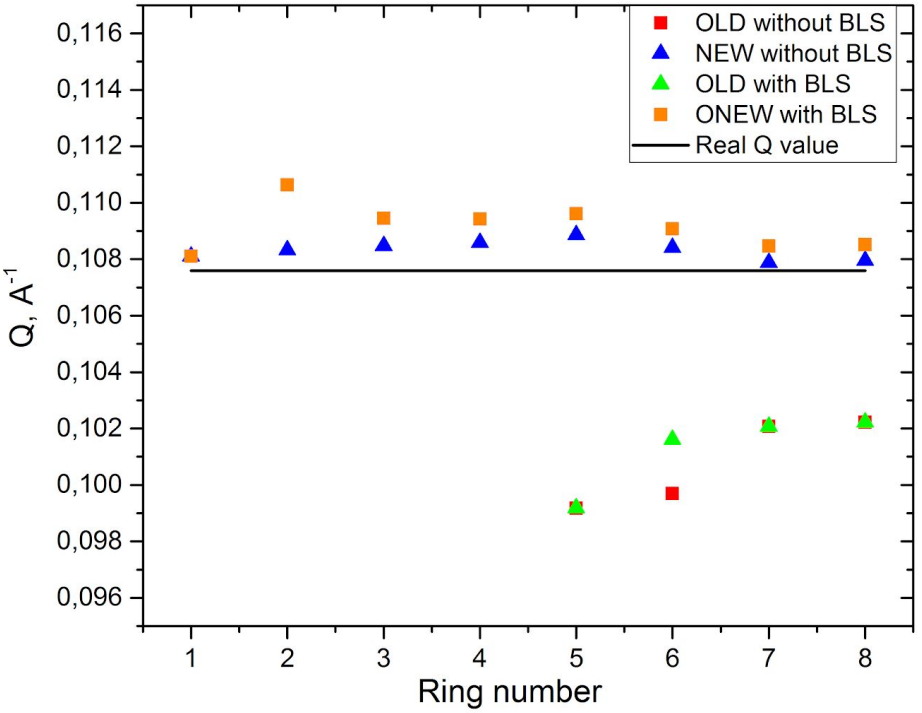

Fig. 9 - Discrepancies between absolute Q value for the 1st Bragg peak of AgBh and detector data.

The "NEW" detector shows the greater discrepancies of Q value in comparison to the "OLD" detector. It should be find the reason of this behaviour. The data from "OLD" detector has smaller deviation and it may be connected only with the use of the central point of each ring for Q value calculation.

Conclusion

Time-of-flight techniques of the YuMO spectrometer were considered in this project, which provide as advantages in the SANS investigations, as set the new problems in the work with data obtained from two detectors, each of them equipped with 8 rings, with the different flight distance and own technical parameters.

The SANS data processing was performed in the Origin program with considering the Maxwell spectra distribution of neutron impulse from the reactor. The Baseline was subtracted for each channel to align the background, the diffraction peaks were fitted by Gaussian form. Conversion of measured values of the Bragg peak was calculated on the different times of flight and, consequently, on different wavelengths. On this basis the transition to the reciprocal space was performed for the scattering pattern of the silver behenate powder standard.

Using theoretical consideration and known facility parameters the program on the Python language was written which executes the conversion of the TOF coordinates into the Q-space. The Q values were obtained for the first Bragg peak on each ring of the both detectors. These peaks were observed, compared and averaged, the error values were calculated for each ring.

This work will help to improve the calculation of the experiment geometry with the changing TOF distances and take into account obtained corrections in the future in the SANS data processing program SAS.

Acknowledgments

I would like to thank a committee of JINR Summer Student Program for allowing me to participate in that science project.

I express my great gratitude to my supervisor A.I. Kuklin for the competent formulation of the scientific task, for the help in the implementation of this project, control and support during the whole student program, for his welcome, introduction into the work of reactor IBR-2, time-of-flight method, experience in the high-pressure PVT-camera work, SANS data processing programs and theoretical model constructions on the experiment data basis.

Thank to my colleague at laboratory of neutron physics V.V. Skoy for the introduction into the theory and useful practical skills with the work connected with lipid core shells and vesicles, for the experience in extrusion and densitometry, for the excursion in the JINR museum.

And thank to my co-worker Alina for the inspiration.

References

1. Wüthrich K. NMR with Proteins and Nucleic Acids // Europhys. News. 1986. Vol. 17, № 1. P. 11–13.
2. Dauter Z., Lamzin V.S., Wilson K.S. Proteins at atomic resolution // Curr. Opin. Struct. Biol. 1995. Vol. 5, № 6. P. 784–790.
3. Kennard O., Hunter W.N. Single-Crystal X-Ray Diffraction Studies of Oligonucleotides and Oligonucleotide–Drug Complexes // Angewandte Chemie International Edition in English. 1991. Vol. 30, № 10. P. 1254–1277.
4. Svergun D.I., Koch M.H.J. Small-angle scattering studies of biological macromolecules in solution // Rep. Prog. Phys. 2003. Vol. 66, № 10. P. 1735–1782.
5. Mertens H.D.T., Svergun D.I. Structural characterization of proteins and complexes using small-angle X-ray solution scattering // J. Struct. Biol. 2010. Vol. 172, № 1. P. 128–141.
6. Jacrot B. The study of biological structures by neutron scattering from solution // Rep. Prog. Phys. 1976. Vol. 39, № 10. P. 911–953.
7. Sears V.F. Neutron scattering lengths and cross sections // Neutron News. 1992. Vol. 3, № 3. P. 26–37.
8. Kuklin A.I., Kh. Islamov A., Gordeliy V.I. Scientific Reviews: Two-Detector System for Small-Angle Neutron Scattering Instrument // Neutron News. 2005. Vol. 16, № 3. P. 16–18.
9. Kuklin A. et al. Past and present of time-of-flight small-angle neutron scattering at IBR-2 // J. Phys. Conf. Ser. 2012. Vol. 351. P. 012001.
10. Ostanevich Y.M. Time-of-flight small-angle scattering spectrometers on pulsed neutron sources // Makromol. Chem. Macromol. Symp. 1988. Vol. 15, № 1. P. 91–103.
11. Soloviev A.G. et al. SAS program for two-detector system: seamless curve from both detectors // J. Phys. Conf. Ser. 2017. Vol. 848. P. 012020.
12. Nyam-Osor M. et al. Silver behenate and silver stearate powders for calibration of SAS instruments // J. Phys. Conf. Ser. 2012. Vol. 351. P. 012024.
13. Ruijter J.M. et al. Amplification efficiency: linking baseline and bias in the analysis of quantitative PCR data // Nucleic Acids Res. 2009. Vol. 37, № 6. P. e45.
14. Ruckstuhl A.F. et al. Baseline subtraction using robust local regression estimation // J. Quant. Spectrosc. Radiat. Transf. 2001. Vol. 68, № 2. P. 179–193.